REPORT DOCUMENTATION PAGE

Form Approved
OMB No. 0704-0188

1. REPORT DATE *(DD-MM-YYYY)*	2. REPORT TYPE	3. DATES COVERED *(From - To)*
Sep 1993	Technical Paper	

4. TITLE AND SUBTITLE

(See attached)

5a. CONTRACT NUMBER

5b. GRANT NUMBER

5c. PROGRAM ELEMENT NUMBER

6. AUTHOR(S)

(See attached)

5d. PROJECT NUMBER
3058

5e. TASK NUMBER
00C4

5f. WORK UNIT NUMBER

7. PERFORMING ORGANIZATION NAME(S) AND ADDRESS(ES) AND ADDRESS(ES)

(See attached)

8. PERFORMING ORGANIZATION REPORT NUMBER

AIAA 93-1901

9. SPONSORING / MONITORING AGENCY NAME(S) AND ADDRESS(ES)

Air Force Research Laboratory (AFMC)
AFRL/PRS
5 Pollux Drive
Edwards AFB CA 93524-7048

10. SPONSOR/MONITOR'S ACRONYM(S)

11. SPONSOR/MONITOR'S REPORT NUMBER(S)
PL-TP-93-3029

12. DISTRIBUTION / AVAILABILITY STATEMENT

(See attached)

DISTRIBUTION STATEMENT A
Approved for Public Release
Distribution Unlimited

13. SUPPLEMENTARY NOTES

These are technical papers, presentations that have been presented by AFRL/PRS from 1994.
AIAA/SAE/ASME/ASEE 29th Joint Propulsion Conference and Exhibit, 13-16 Sep, Monterey, CA

14. ABSTRACT (maximum 200 words)

(See attached)

15. SUBJECT TERMS

16. SECURITY CLASSIFICATION OF:			17. LIMITATION OF ABSTRACT	18. NUMBER OF PAGES	19a. NAME OF RESPONSIBLE PERSON
a. REPORT	b. ABSTRACT	c. THIS PAGE			Kenette Gfeller or Leilani Richardson
Unclassified	Unclassified	Unclassified	SAR		19b. TELEPHONE NUMBER *(include area code)* DSN 525-5015 or 525-5016

AIAA 93-1901
An investigation of the Breakdown Voltage Characteristics of a 30 kW Class Ammonia Arcjet

D.L. Tilley, K.A. McFall, S. Castillo, and J.C. Andrews
Phillips Laboratory
Edwards AFB, CA

D.R. Bromaghim
SPARTA, Inc.
Phillips Laboratory
Edwards AFB, CA

AIAA/SAE/ASME/ASEE
29th Joint Propulsion Conference and Exhibit
June 28-30, 1993 / Monterey, CA

AN INVESTIGATION OF THE BREAKDOWN VOLTAGE CHARACTERISTICS OF A 30 KW CLASS AMMONIA ARCJET

D.L. Tilley*, D.R. Bromaghim†, K.A. McFall*, S. Castillo‡, J.C. Andrews§
Electric Propulsion Laboratory
Phillips Laboratory
Edwards A.F.B., CA 93524

Abstract

The primary objective of this work was to identify methods to reduce the mean dynamic breakdown voltage (MDBV) of the ammonia propellant in the ESEX 26 kW arcjet. The approach to this objective was to establish a test matrix to investigate the influence of mass flow rate, electrode gap distance, cathode tip shape, and voltage ramp rate on the MDBV. Only the mass flow rate and voltage ramp rate were observed to significantly affect the MDBV; the MDBV was observed to rise as either of these parameters were increased. These test results provided the basis for the start circuit redesign for the ESEX flight experiment, and also represent an initial data base of breakdown characteristics in high power ammonia arcjets. The second objective of this work was to identify the mechanisms associated with propellant breakdown in an arcjet. Progress towards this objective includes the following. A framework for investigating breakdown mechanisms in an arcjet was established which provides explanations for the strong dependence of the MDBV on the voltage ramp rate, the mass flow rate, and other parameters. A combination of a model, the calculation of electric field contours inside of the arcjet, and SEM photographs of a cathode tip indicate that the projection model for enhance field emission cannot alone account for the mean dynamic breakdown voltages observed in the high power arcjet. This result suggests that dielectric surface layers on the cathode tip are responsible for the enhanced field emission required to explain the observed MDBVs.

I. Introduction

A reliable ignition method is essential for the space qualification of an arcjet propulsion system. Arcjets are most commonly ignited by applying a high voltage pulse across the electrodes to breakdown the propellant. Following breakdown, the arcjet rapidly (on the order of 100's of microseconds) transitions into a steady state high power arc. This study will focus on the initial phase of arcjet ignition: propellant breakdown. In particular, this study is concerned with the breakdown characteristics of a 30 kW class arcjet operating on ammonia.

The motivation for this work originated from the difficulty in designing a reliable arcjet start circuit for the USAF Electric Propulsion Space Experiment (ESEX). ESEX is a flight experiment of a 26 kW arcjet propulsion system, with the objective of resolving many of the spacecraft integration issues associated with the arcjet system[1]. Supported by some experimental data, the original start circuit design was based on the assumption that a 1 to 2 kV pulse would readily breakdown the ammonia propellant[2]. Experiments at the Rocket Research Company showed that this assumption was not correct, and that a better characterization of the breakdown voltage in the 30 kW class ammonia arcjet was needed. The main objective of this work was to furnish the data required to redesign the ESEX start circuit by identifying methods to reduce the breakdown voltage. The approach to this objective was to investigate the influence of cathode tip shape, electrode gap setting, mass flow rate, and voltage ramp rate on the breakdown voltage in an 30 kW ammonia arcjet. This work will also serve as an initial data base for the breakdown characteristics in high power ammonia arcjets, because past arcjet breakdown research has been limited to 1 kW class arcjets[3,4]. Such a data base will serve to facilitate the design of start circuits of future ammonia arcjets to be operated in space at the 10-30 kW power level, such as the arcjet(s) to be operated on the flight experiment ELITE[1].

Previous investigations of propellant breakdown in an arcjet were empirical in nature[3,4]; no attempt to identify the breakdown mechanisms has been made. Understanding these mechanisms has become increasingly important as start circuits are being developed for arcjets of various dimensions and propellants. Many non-intuitive problems have hampered the start circuit designer, such as the sensitivity of the breakdown voltage to the voltage ramp rate and to cathode surface layers. The difficulty in designing a robust start circuit is further illustrated by a recent cyclic endurance test of a 30 kW class ammonia arcjet operating at 10 kW[5]. In this 707 cycle test, the arcjet typically started on the first voltage pulse at a breakdown voltage of about 3 kV. However, on one occasion, 56 pulses with peak voltages as high as 4.6 kV were required before propellant breakdown occurred. On another occasion, 25 attempts were required to breakdown the propellant. Difficulties in propellant breakdown have also been documented elsewhere[6-8].

An arcjet ignition research program has been established at the Phillips Laboratory with the primary objective of identifying the breakdown mechanisms in all arcjets. The approach to this objective is to develop a model to predict the breakdown voltage, in an attempt to explain the above observations and other non-intuitive phenomenon seen. The modelling work, which will be discussed in detail in a future paper[9], is currently in progress, but some preliminary aspects will be discussed in this paper. In this study, a portion of the model, SEM photographs of the cathode tips, and the calculation of electric field contours

---

* Research Engineer, Member AIAA
† Engineer, SPARTA, Inc., Member AIAA
‡ Capt. USAF, Member AIAA
§ Former Group Leader, Member AIAA

inside of the arcjet will be used to investigate the electron emission processes from the cathode.

This research is expected to benefit the design of arcjets and arcjet start circuits to improve the reliability of arcjet ignition in space. Possible benefits include: the identification of arcjet design changes to improve breakdown characteristics without affecting performance, the identification of facility effects associated with obtaining breakdown characteristics in vacuum chambers, the identification of environmental effects associated with the ground handling of a space-bound arcjet, and the minimization of adverse interactions between the starting circuit and the power processing unit. In addition, there are many arcjet ignition/spacecraft interaction issues which are affected by arcjet starting: EMI associated with ignition, propellant loss during the starting process, and spacecraft torques due to the mistiming of igniting arcjet pairs.

The paper is organized as follows. In section II, the experimental apparatus, test matrix, and procedures are discussed. The experimental results are presented in section III. A preliminary investigation of breakdown mechanisms in an arcjet is presented in section IV. In section V, a model developed in section IV is used to investigate the electron emission process from the cathode in the high power ammonia arcjet. Conclusions are discussed in section VI.

II. Experimental Apparatus/Test Matrix

Experimental Apparatus

The arcjet used in this study, shown in figure 1, is a modified version of the D-1E 30 kW arcjet[10] and is described in detail elsewhere[11]. The constricter and nozzle dimensions were identical to those in the ESEX flight arcjet. The constricter had a diameter of 3.81 mm (0.15 inch) with a length to diameter ratio of one; the conical nozzle had a 40:1 area ratio with a half angle of 19 degrees. The cathode was made of 2% thoriated tungsten; the pure tungsten anode nozzle remained in its newly machined state throughout testing. The electrode gap distance was set by first sliding the cathode into the chamber until it contacted the anode. The electrode gap distance is defined as that distance the cathode is then withdrawn from the anode. The uncertainty of the electrode gap distance was less than 7.62×10^{-3} cm (0.003 in.).

The anhydrous ammonia propellant (99.99% pure) was fed from a bottle placed on a scale, through a Micro Motion mass flow meter (model D6) to the arcjet. The mass flow meter was calibrated before testing began, and shown to have an uncertainty of less than 2% at all of the mass flow rates used in this study. The calibration matched the factory calibration, and others performed previously with different propellants. Between the mass flow meter and the arcjet, outside of the vacuum chamber, was a pressure gauge and a 5000 torr full scale capacitance manometer (MKS Instruments, Inc.). The capacitance manometer measured the feed pressure with an uncertainty of approximately 0.5%. The mass flow rate was adjusted with two meter valves connected in parallel upstream of the mass flow meter.

Tests were performed in the Electric Propulsion Laboratory at the Phillips Laboratory at Edwards AFB, CA in test chamber number 1. This stainless steel cylindrical chamber is 1.8 m in diameter, 2.4 m long, and is evacuated by two pumping trains capable of a total volumetric flow rate of 11000 liters/sec (23000 CFM). The vacuum pressure was measured with a Varian model 531 thermocouple gauge with a Varian model 801 thermocouple gauge controller. With no flow, this system is capable of maintaining vacuum pressures of less than 5 mtorr, and at a mass flow rate of 240 mg/sec of ammonia, the maximum for these tests, the vacuum pressure is less than 100 mtorr. During the breakdown characterization tests, due to various leaks and the use of only one pumping train at times, the maximum vacuum pressure reached 250 mtorr at 240 mg/sec ammonia.

The experimental set up for the breakdown characterization tests is shown in figure 2. The voltage pulse to the arcjet was supplied by a Pacific Electro Dynamics designed start circuit, which will be described later. The arcjet was placed such that the nozzle faced a 0.5 m diameter window located about one meter from the arcjet. This configuration provided optical access to the constricter region of the arcjet, allowing visual conformation of breakdown in the arcjet. The anode and cathode voltage with respect to ground were measured with Tektronix P6015 1000:1 voltage probes. These probes were calibrated and compensated before

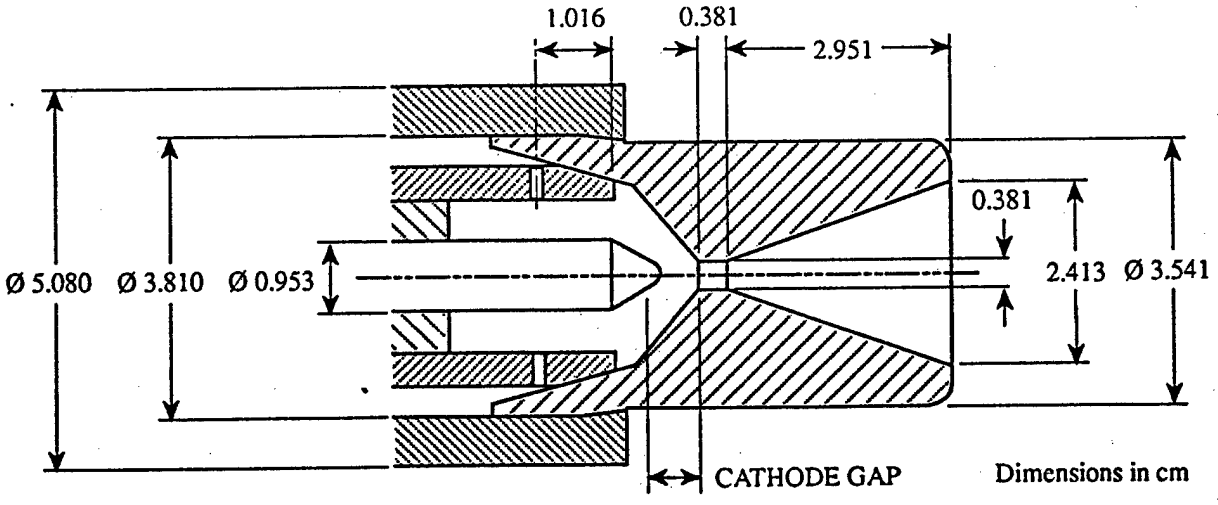

Figure 1: A schematic of the modified version of the D-1E 30 kW arcjet

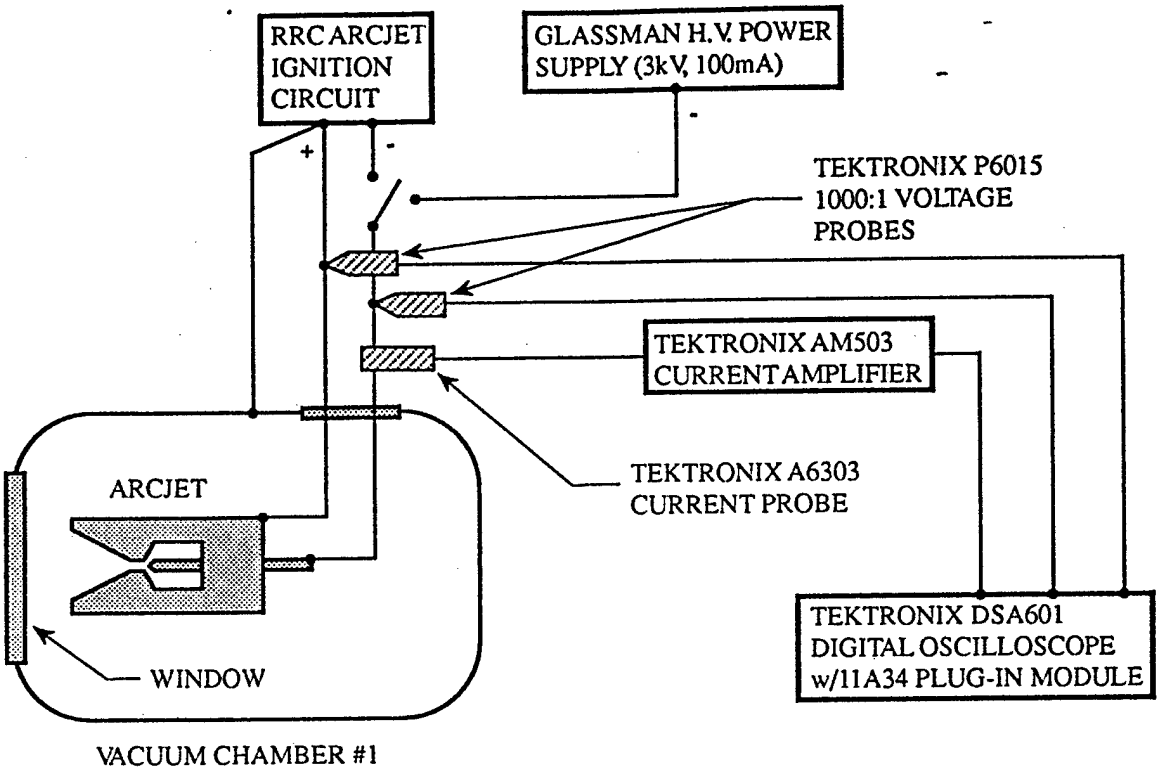

Figure 2: A schematic of the experimental set up.

testing began; the uncertainty in the voltage measurements was approximately 5%. Also note that the measurement of voltages at the start circuit box were experimentally observed to be identical to those at the arcjet. The current through the circuit was measured with a Tektronix A6303 current probe with a Tektronix AM503 current amplifier. All signals from the voltage and current probes were measured with a Tektronix DSA601 digital oscilloscope with a 11A34 plug-in module. The oscilloscope could only sample two of the three signals at one time, with a maximum sampling rate of 500 MHz. Finally, a Glassman high voltage power supply (Model ER3R100, 3 kV, 100 mA) was configured such that it could be switched into the circuit for cathode conditioning purposes and for measuring the mean static breakdown voltage. The cathode conditioning process will be discussed in more detail later.

The Pacific Electro Dynamics designed start circuit is based[12] on those designed for 1 and 10 kW arcjets[3,4,8]. Typical open circuit pulses produced by the start circuit are shown in figure 3. The risetime, duration, and magnitude of the voltage pulse could be changed by placing various capacitors across the output of the start circuit. The rise of the voltage pulse was essentially linear, and breakdown always occurred while the voltage was rising. After breakdown, the start circuit is capable of powering an arc at 10 to 20 amps for about a tenth of a millisecond. This capability allows the PPU time to transition to the steady state arc associated with normal arcjet operation; although, in all of these tests, this transition did not occur because the main power supply was disconnected from the arcjet. Figure 4 shows a sample measurement of the voltage and current to the arcjet during a breakdown event. Breakdown occurs at approximately 3 kV, afterwards the start circuit is observed to supply a 15 A current to the arcjet. Note that the measurement of initial fluctuations in current is dominated by noise pick up, and does not represent actual current fluctuations.

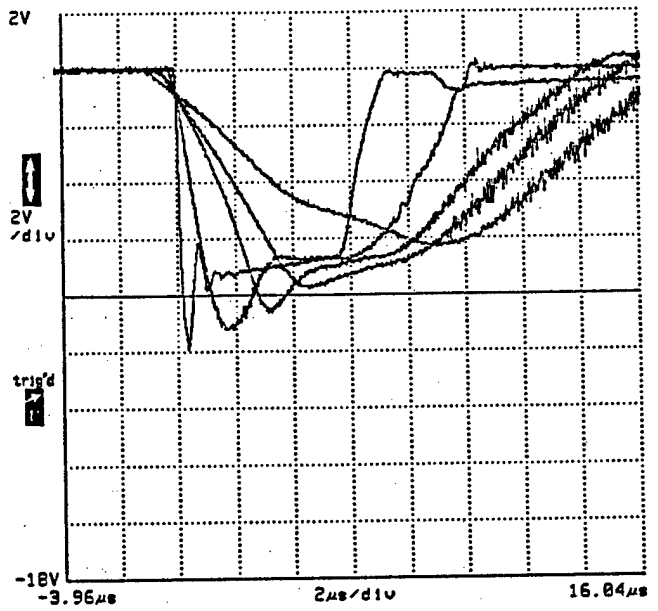

Figure 3: Open circuit voltage wave forms from the Pacific Electro Dynamics start circuit (vertical scale is 2 kV/div; horizontal scale is 2 µsec/div)

Test Matrix

In the first series of tests, both the mean static breakdown voltage (MSBV) and mean dynamic breakdown

voltage (MDBV) were measured as a function of mass flow rate, electrode gap distance, and cathode tip shape. In these tests, a voltage pulse slightly different than the fastest rising pulse shown in figure 3 was used (9 kV peak, 4 µsec duration, 25 kV/µsec rise rate). Three mass flow rates were used: 70, 120, 240 mg/sec; where 240 mg/sec represents the full flow condition for the arcjet to be flown on ESEX. Three electrode gap distances were used: 0.38 cm (0.15 in.), 0.48 cm (0.19 in.), 0.61 cm (0.24 in.); where 0.61 cm represents that on the ESEX flight unit. The range of electrode gap distance is small, but was considered the maximum variation possible to avoid significantly altering arcjet performance. Five different cathode tips were used in this study. These were labeled the sharp tip, flat tip, round tip, burned-in cathode #1 and #2. The dimensions of the first three are shown in figure 5. Burned-in cathode #1 and #2 had been fired for greater than 10 hours at 10-30 kW, and were used to represent actual cathodes in the breakdown tests. Burned-in cathode #1 was used in a limited number of tests to compare data with Rocket Research Company results and to briefly investigate the effect of cathode surface contaminants. The rational behind the variation of cathode tip shape was to investigate the electric field concentrating effect on the breakdown voltage. Finally, a follow-up experiment to the above test matrix was performed to investigate the effect of voltage ramp rate on the MDBV for an arcjet operating at the mass flow rate and electrode gap distance in the ESEX arcjet.

Procedure

Once configured in the desired geometry, and the arcjet leak tested, the cathode was conditioned at the lowest flow rate (70 mg/sec) with the high voltage power supply. This process was performed in an effort to negate the effect of cathode surface layers, due to handling, on the MDBV. This was accomplished by operating the power supply for 10 minutes in a mode where it would produce propellant breakdowns at a rate on the order of 100 Hz. Note that this mode is different than operating the power supply with a series resistor to produce a stable glow discharge. The 100 Hz breakdown process was observed to produce reproducible breakdown voltages, except for one anomalous case. The conditioning process was performed anytime the vacuum chamber was opened and then closed, i.e. when the electrode gap distance was set or cathode replaced.

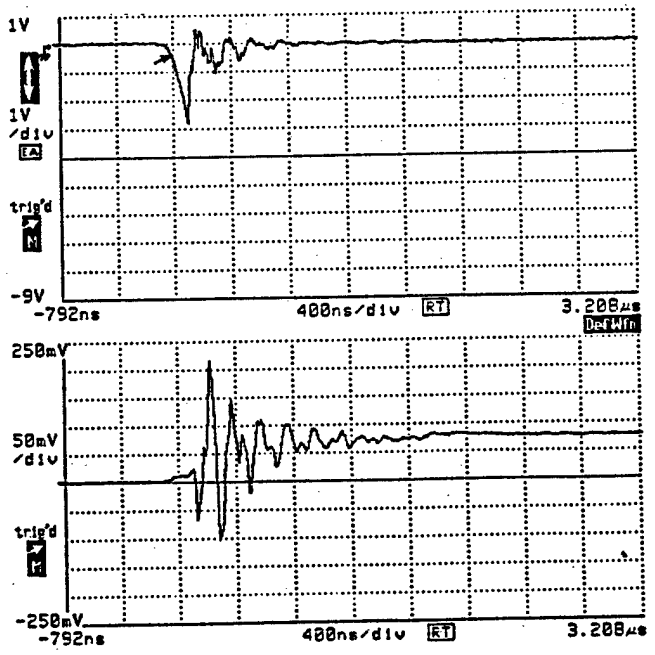

Figure 4: A typical voltage (above, vertical scale is 1 kV/div) and current (below, vertical scale is 10 A/div) measurement associated with a breakdown event (horizontal scale is 400 nsec/div).

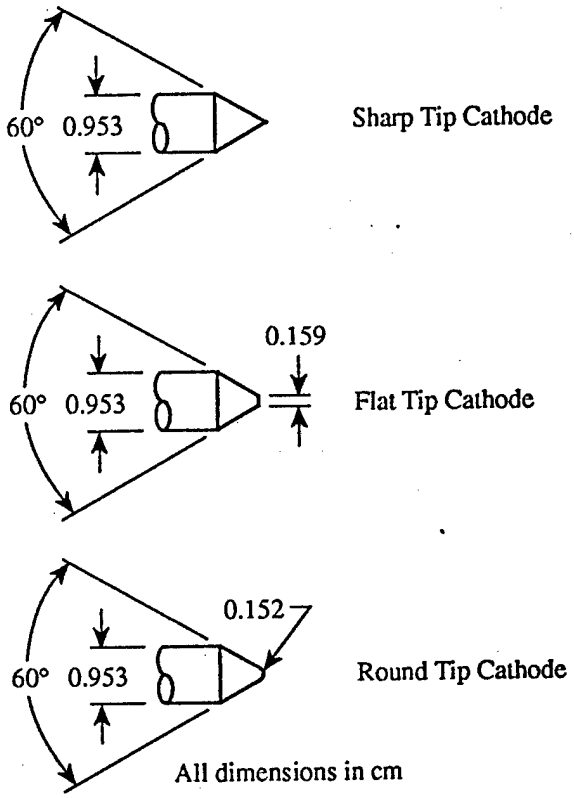

Figure 5: Machined cathode dimensions prior to testing (drawing not to scale).

After the conditioning process, the cathode was allowed to cool down for about five minutes. Then the static breakdown voltage measurements were obtained. This was accomplished by slowly raising the voltage to the electrodes by hand, at a rate on the order of 50 V/sec, until breakdown occurred. Typically this was repeated at least three times for repeatability and/or to characterize the variation in the static breakdown voltage. The static breakdown voltage was measured at the three mass flow rates. After these tests, the start circuit was switched into the circuit such that the dynamic breakdown voltage measurements could be obtained. A total of 20 measurements were taken at each operating location to characterize both the MDBV and the range of variation. A duration of at least 15 seconds was maintained between each breakdown voltage measurement, to eliminate cathode heating effects[4].

III. Experimental Results

Ammonia Arcjet Breakdown Characteristics

The breakdown characteristics of the various cathode tips are shown in figures 6-9. Plotted is the MDBV versus the mass flow rate, $\dot{m}$, of ammonia at various electrode gap distances, d. All of these tests were conducted with the voltage pulse with the ramp rate of 25 kV/μsec. The standard deviation of the sample of breakdown voltages is indicated by the error bars. Comparisons of the breakdown characteristics of the different cathode tip shapes indicate that the tip shape does influence the MDBV, but it does so in an apparently unpredictable way. This behavior will be discussed further in section V. The electrode gap distance was also observed to not significantly affect the MDBV. The comparison of these results with breakdown characteristics taken in 1 kW arcjets[3,4] suggest that this is due to the small variation in electrode gap setting. As with the 1 kW arcjet breakdown characteristics, the mass flow rate did have a significant effect on the MDBV for all cathode tip shapes.

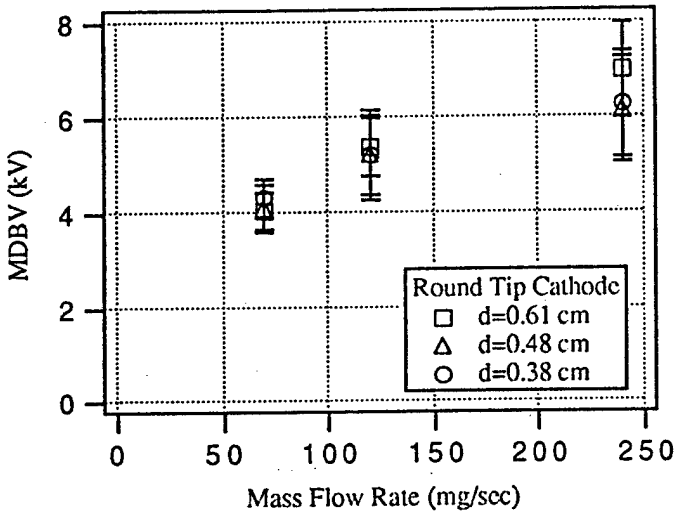

Figure 6: The breakdown voltage characteristics of the round tip cathode.

The Effect of Voltage Ramp Rate

Voltage ramp rate effects were first examined by investigating the limiting case where the voltage ramp rate is practically zero (i.e., the mean static breakdown voltage). Shown in figure 10 is the MSBV versus the product of the electrode gap distance and the mass flow rate, which is expected to be proportional to the feed pressure (p_{feed} [Pa] = 280.5 $\dot{m}$[mg/sec]) and the pressure inside of the arcjet. It is first noted that the MSBVs are significantly lower than the MDBVs for all cathode tip shapes. Furthermore, MSBV characteristics of all of the cathode tip shapes essentially obeyed Paschen's Law (i.e. $V_{bo}=V_{bo}(pd)$ only), although the variation of the MSBV with cathode tip shape is very peculiar. Burned-in cathode #2 and the flat tip cathode appear to follow the same curve, while the sharp tip cathode and burned-in cathode #1 follow a different curve. The round tip cathode appears to transition between the respective curves.

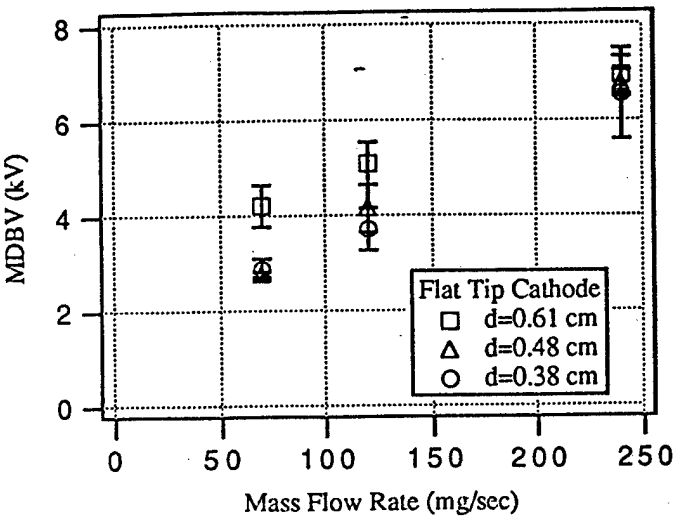

Figure 7: The breakdown voltage characteristic of the flat tip cathode.

This phenomenon is unexplained as of now, but is perhaps linked to the complicated flow injection scheme in this arcjet, where the flow is possibly supersonic inside of the arcjet. Assuming that the flow is choked at the four injection holes, these curves also compare favorably (within a factor of 2) with static breakdown voltage data for ammonia obtained between two flat plates[13].

From past experiments with 1 kW arcjets[3,4], preliminary tests at the Phillips Laboratory with a NASA LeRC 10 kW PPU start circuit (Voltage ramp rate ~1 kV/msec)[14], and the static breakdown voltages shown in figure 10, indicated that the best approach to significantly reduce the MDBV was to significantly reduce the voltage ramp rate. Reducing the ramp rate did indeed lower the MDBV as shown in figure 11. These tests were performed with the burned-in cathode #1 at the ESEX configuration (240 mg.sec, d=0.61 cm). The effect of ramp rate on the

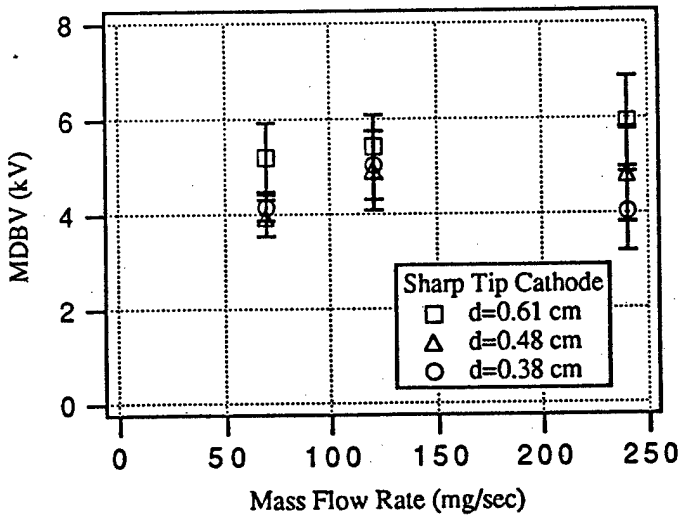

Figure 8: The breakdown voltage characteristic of the sharp tip cathode.

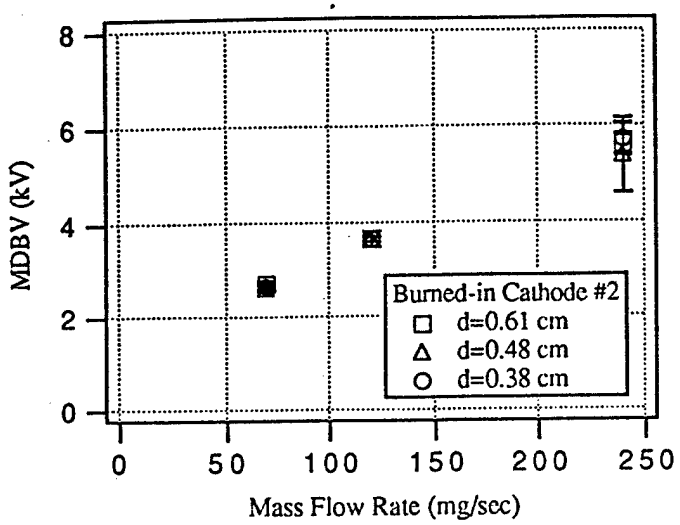

Figure 9: Breakdown voltage charcteristics of burned-in cathode #2.

MDBV in this arcjet is also corroborated by the comparison of figures 6-9 to data obtained in the cyclic endurance test discussed previously ($V_b \equiv 3$ kV, $V' \equiv 3$kV/µsec, $\dot{m}$=170 mg/sec)[15]. The results of these tests were incorporated in the new ESEX start circuit design.

Anomalies/The Effect of Contaminants

In this section, the effect of cathode surface contaminants will be briefly discussed, along with the reporting of two observed anomalies which are most likely related to surface layers on the cathode. Two breakdown characteristics are shown in figure 12, corresponding to before and after the cathode was conditioned. This figure indicates that the cathode surface state is very important to the mechanisms that affect the MDBV. In most cases cathode conditioning was observed to raise the MDBV, but not always. After the conditioning process, MDBV measurements were observed to be repeatable except for one anomaly. This incident occurred after the conditioning of the flat tip cathode. The initial measurement (at 120 mg/sec and d=0.38 cm) of the MDBV was 5.4 ± 0.6 kV. After obtaining the MDBV at 70 mg/sec, the 120 mg/sec measurement was repeated to be 3.7 ± 0.4 kV, which is the value in figure 7.

Another anomaly was the discrepancy between the MDBV of burned-in cathode #1, at 240 mg/sec and d = 0.61 cm, measured at different times throughout this research. The first measurement is shown in figure 12 to be 6 ± 1.3 kV. The later measurement with the same cathode is shown in figure 11, indicating a MDBV of 7.9 ± 1.5 kV. This difference may be linked to a few hours of work to characterize the conditioning process just prior to the MDBV

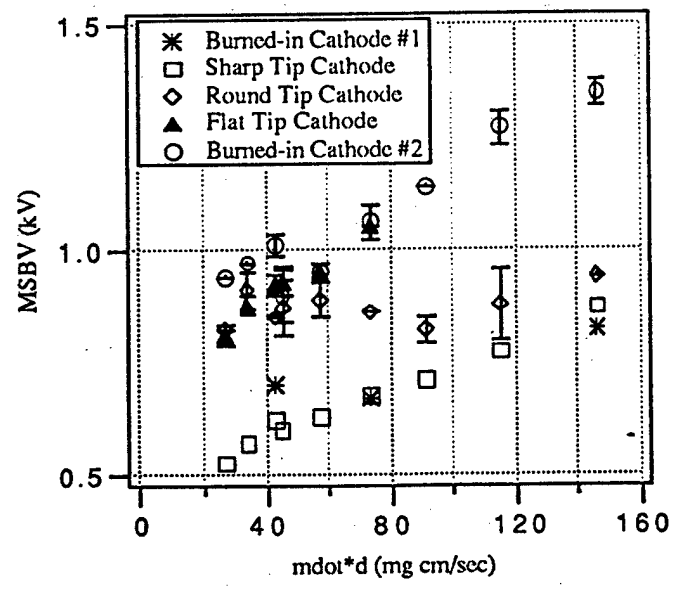

Figure 10: Static breakdown voltage characteristics of all cathode tip shapes

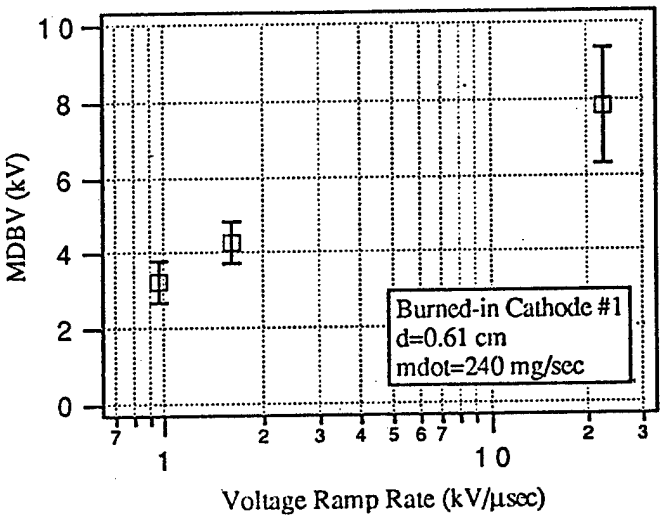

Figure 11: Effect of voltage ramp rate on the MDBV of burned-in cathode #1

measurements of figure 11. It is obvious that more research is required to investigate the various conditioning processes for reproducibility and the simulation of the actual cathode surface state in the space environment.

IV. A Preliminary Investigation of Breakdown Mechanisms in an Arcjet

In the first part of this section, a framework for investigating propellant breakdown mechanisms in an arcjet is discussed, followed by more detailed treatments of each of its components. Nearly all arcjet start circuits to date use a voltage profile which increases essentially linearly until breakdown occurs. Qualitatively, it is expected that the MDBV, V_b, can be described by the equation shown below:

$$V_b \sim V_{bo} + V'(t_s + t_f) \qquad (1)$$

where V_{bo} is the mean static breakdown voltage, V' is the voltage ramp rate in Volts/sec, and t_s and t_f are the mean statistical and formative time lags respectively. The mean statistical time lag, t_s, is the time required for a free electron

to appear, preferably near the cathode, by processes such as electron field emission, photoelectric effect, and propellant ionization due to cosmic rays and/or nearby radioactive sources. The mean formative time lag is the average time, after an electron has been emitted from the cathode, for propellant breakdown to actually occur. The natural scatter in the data, shown in section III, is the result of the fact that all of the parameters discussed above are fundamentally random phenomena.

It is important to emphasize that equation 1 can only be used for order of magnitude estimates of the MDBV. Only if t_s and t_f were both independent of the instantaneous voltage, could the "approximate sign" in equation 1 be replaced with an "equal sign." Unfortunately, the mean statistical and formative time lags are usually strong functions of the voltage; in which case, equation 1 is ill-defined. More detailed models are then required to accurately predict the MDBV.

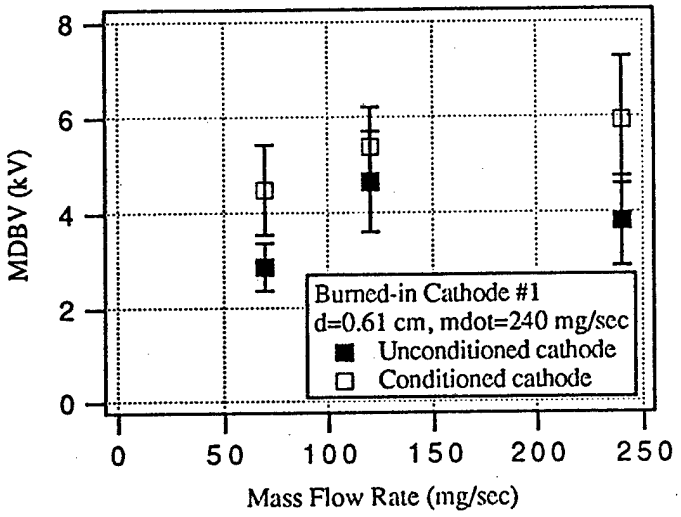

Figure 12: The effect of cathode conditioning on the MDBV of burned-in cathode #1.

With equation 1 in mind, the mechanisms responsible for the production of the initial electron (t_s) and for breakdown formation (t_f) are discussed. Although most of these discussions are applicable to all arcjets, the focus in this paper will be on those processes applicable to the ground testing of the high power ammonia arcjet. The breakdown mechanisms in 1 kW arcjets will be discussed in a later paper[9].

The Determination of the Mechanism Responsible for Initial Electron Production

When an arcjet is ground tested, the dominant source of free electrons is electron field emission from the cathode. This is also the case for essentially all electrical breakdown studies[16,17]. Furthermore, the assumption that either cosmic rays and/or radioactive sources are the dominant electron source is not consistent with the strong effect that cathode surface layers have on the MDBV. The electron production rate by photoelectric effect is also expected to be negligible at room temperature[16]. Further investigation is required to determine if electron field emission is dominant in the space environment.

As an alternative to calculating the mean statistical time lag, it is of more interest to calculate V_o, the average voltage at which an electron is emitted from the cathode surface. Such a parameter is used in a model for the MDBV[9], which is formulated such that the MDBV is a function of V_o and those parameters which affect breakdown formation. In equation 1, V_o can be considered equal to $V_{bo} + V't_s$. It is also assumed that only one electron is required to initiate the avalanche process leading to propellant breakdown. This is a good assumption when applied to the arcjet breakdown process, because in general V_b is significantly greater than V_{bo}. As V_b approaches V_{bo}, the probability that a single electron will initiate breakdown deviates significantly from unity[16].

To derive an expression for V_o, it is first helpful to introduce the characteristic time of the ramping profile, t_r, defined as:

$$t_r = \frac{V - V_{bo}}{V'} \qquad (2)$$

Note that t_r is defined such that it is equal to zero when the voltage V is equal to V_{bo}, denoting that only when the voltage is greater than the MSBV will an emitted electron initiate breakdown. As will be shown later, the mean statistical time lag is an extremely strong function of the voltage ($t_s \sim V^{-2}\exp[\text{const.}/V)]$). As the voltage is increasing, the characteristic ramp time is increasing ($t_r \sim V$) and the mean statistical time lag is decreasing such that when $t_r \sim t_s$ it is expected that on the average an electron will be emitted from the cathode. By assuming that on the average an electron is emitted when $t_r(V_o) = t_s(V_o)$, V_o can be determined from the following equation:

$$t_s(V_o) = t_r(V_o) = \frac{V_o - V_{bo}}{V'} \qquad (3)$$

It will be shown later that any constant on the order of one multiplied to one side of the above equation, has a small effect on V_o.

Such a relation for determining V_o is analogous to the Bray criterion[18] used to predict the location of the freezing point in a nozzle. Bray suggested that because the characteristic flow time is rapidly decreasing and the characteristic recombination time is rapidly increasing, the location where the flow transitions from equilibrium to frozen flow is the position in the nozzle where $t_{flow} \sim t_{recomb}$. Such a model compared with more accurate calculations very favorably.

It can be shown that the mean statistical time lag is inversely related to the number of electrons emitted from the cathode per unit second[16]:

$$t_s = \frac{1}{\frac{1}{e}\int J\,dA} \qquad (4)$$

where e is the electron charge and J is current density of electrons emitted from the cathode surface. This current density, J, is assumed to be due to field emitted electrons, described by the following equation[19-21]:

$$J = \frac{\pi\kappa}{\sin(\pi\kappa)} \frac{1.54\times10^{-6}}{\phi t^2(y)} E^2 \exp\left(\frac{-6.83\times10^7\phi^{3/2}v(y)}{E}\right) \quad [A/cm^2] \qquad (5)$$

where:

$$y = 3.79\times10^{-4}\frac{E^{1/2}}{\phi} \qquad \kappa = 8.836\times10^3\frac{T\phi^{1/2}t(y)}{E}$$

and v(y) and t(y) are smooth functions tabulated in reference 22, ranging from zero to one. Note that for the above expressions, the local electron field E must be expressed in Volt/cm, the cathode work function, ϕ, in eV, and temperature T in K. Also note that as $T\rightarrow0$, equation 5 reduces to the Fowler-Nordheim equation[19-21] for electron field emission from a perfectly smooth surface. The criterion for the applicability of equation 5 is[19]:

$$7.6\times10^6\phi^2 > E\ [\text{Volt/cm}] \geq 1.22\times10^4\phi^{1/2}T \qquad (6)$$

The integration of equation 5 over the surface of the cathode is practically impossible due to the roughness of the arcjet cathode surface. Therefore, the local electric field is replaced with $\beta\beta_m V/d$, where V is the voltage across the electrodes, d is the electrode gap distance, β is the field enhancement factor, and β_m is the macroscopic field enhancement factor. The field enhancement factor, β, is a standard parameter used in vacuum arc applications[23,24] to account for the enhancement of the electric field at the surface of the cathode due to microscopic surface roughness. The macroscopic field enhancement factor, β_m, accounts for the deviation of the electric field near the cathode tip from the mean field, V/d, due to the cathode and anode geometry. Consistent with the replacement of E with $\beta\beta_m V/d$, the integral of J_{TF} over the cathode surface is replaced with JA_e, where A_e is called the effective emission area[23,24]. These assumptions are required due to the difficulty in modelling the topological features of an electrode and because many times electron field emission from a surface is dominated by a few high-β emission sites. Substituting into equation 4:

$$t_s = \frac{e}{J_{TF}A_e} = 6.49\times10^5\frac{e\phi t^2(y)}{A_c(\beta\beta_m V/d)^2}\frac{\sin(\pi\kappa)}{\pi\kappa}\exp\left(\frac{6.83\times10^7\phi^{3/2}v(y)}{\beta\beta_m V/d}\right) \qquad (7)$$

The factors β, β_m, and A_e are discussed in detail below.

The expression for the mean statistical time lag, equation 7, can be substituted into equation 3 to determine the average voltage at which an electron is emitted from the cathode, V_o:

$$V_o^2(V_o - V_{bo}) = 1.04\times10^{-13}\frac{V'}{A_e}\frac{\sin(\pi\kappa_o)}{\pi\kappa_o}\frac{\phi t^2(y_o)}{(\beta\beta_m/d)^2}\exp\left(\frac{6.83\times10^7\phi^{3/2}v(y_o)}{V_o\beta\beta_m/d}\right) \qquad (8)$$

where κ_o and y_o are evaluated at V_o, and equation 8 is solved by iteration. Plotted in figure 13 is V_o as a function of V'/A_e for various values of $\beta\beta_m/d$, ϕ=3.5 eV, and V_{bo}=900V. This plot shows that V_o weakly dependent on V'/A_e, and an extremely strong function of $\beta\beta_m/d$ (unless V_o is very near V_{bo}). Changes of at least an order of magnitude in the effective emission area and/or the voltage ramp rate are required to affect V_o. This insensitivity also justifies the assumption that a proportionality constant on the order of one multiplied into equation 3 has negligible affect on V_o. Although not shown, V_{bo} also has a weak influence on V_o when V_o is substantial percentage above V_{bo}. The effect of work function is relatively strong, see figure 13, and does provide an over-simplified explanation for the effect of cathode surface layers on the MDBV. The cathode temperature does not seriously affect electron emission for the parameters listed above. Only when $\beta\beta_m V/d$ approaches the lower limit of equation 6 does cathode temperature start to effect electron emission from the cathode. In figure 13, as V'/A_e is reduced, the curves stop (for $\beta\beta_m/d=1\times10^3$/cm and 5×10^3/cm) as the lower limit of applicability is encountered.

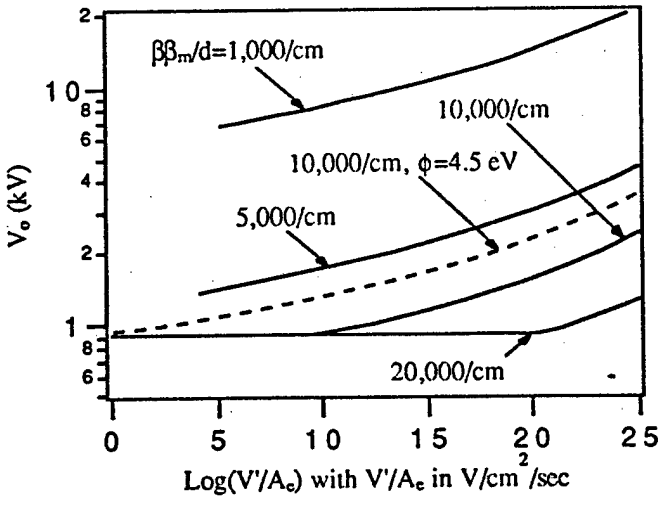

Figure 13: The effect of V'/A_e on V_o for various $\beta\beta_m/d$ (V_{bo}=900 V, T=298 K, ϕ=3.5 eV except as noted).

Breakdown Formation Mechanisms

Once an electron appears from the cathode, there are many different mechanisms by which breakdown may occur in the arcjet. In principle, the mechanism can vary from arcjet to arcjet, depending on its dimensions, the mass flow rate, propellant type, etc. In fact, the investigation of breakdown mechanisms between two flat plates is also a

topic of current electrical breakdown research[17]. In this section, only an initial discussion of the breakdown mechanisms is presented. This will be helpful in the analysis of the ammonia arcjet breakdown data; however, a more detailed analysis of propellant breakdown in this arcjet was not performed due to the lack of fundamental data for ammonia.

Most breakdown mechanisms can be split into two categories: Townsend mechanisms and streamer mechanisms. The rate at which breakdown occurs for a Townsend process depends on the source of the secondary electrons, required for the continued exponential growth of current, leading to breakdown. Different sources of secondary electrons may have drastically different formation times. For example, when ion bombardment is the dominant source of secondary electrons, the formative time lag is proportional to[17]:

$$t_f \sim \frac{d}{U_i}$$

where d is the electrode gap distance and U_i is the ion drift velocity in the arcjet. Since $U_i \sim E/n \sim V/d\dot{m}$:

$$t_f \sim \frac{\dot{m}d^2}{V} \qquad \text{(Townsend Mechanisms)} \qquad (9)$$

where E and n are the electric field and neutral number density in the arcjet, V is the voltage across the arcjet electrodes, and $\dot{m}$ is the mass flow rate. It will be shown in a later paper[9], that this mechanism is most likely responsible for breakdown in a 1 kW arcjet operating on a hydrazine type mixture of hydrogen and nitrogen[3]. In fact, this mechanism can explain the non-monotonic increase in the MDBV with mass flow rate observed in that study.

Another source of secondary electrons is by photoelectric effect, as photons produced by the decay of excited neutral atoms impinge upon the cathode. Here, the formative time lag may be expressed as[17]:

$$t_f \sim \frac{d}{U_e}$$

where U_e is the electron drift velocity. Since U_e is also proportional to E/n, equation 9 is also applicable to this process, although t_f is much smaller for this case because the electrons drift much more rapidly than ions.

The final formation process considered is the streamer mechanism[17,25]. This mechanism is generally observed in fairly dense gases; the most familiar form of streamer type breakdowns are lightning discharges. A common expression for the formative time lag for streamer processes is[17]:

$$t_f \sim \frac{20}{\alpha U_e}$$

where α is the Townsend first ionization coefficient, which can be fitted to the following functional form of[25]:

$$\alpha \sim n \exp\left(\frac{-\text{const.}}{(E/n)}\right) \sim \dot{m} \exp\left(\frac{-\text{const.}}{(V/d\dot{m})}\right)$$

Thus an expression of the formative time lag in arcjet parameters is:

$$t_f \sim \frac{20}{\frac{V}{d}\exp\left(\frac{-\text{const.}\ \dot{m}}{(V/d)}\right)} \qquad \text{(Streamer Mechanism)} \qquad (10)$$

Although qualitative, equations 9 and 10, along with equation 1, are a much more convincing argument for why the MDBV depends on the mass flow rate than the Paschen's law argument used in previous work. The fact that the MDBV is strongly influenced by the mass flow rate and by the voltage ramp rate indicate that the understanding of the breakdown formation process is crucial in the attempt to model the MDBV in an arcjet.

Although elementary, these equations can be used to quantitatively estimate the MDBV for each of the mechanisms, to get an idea of which may be responsible for breakdown in the 30 kW class ammonia arcjet. Unfortunately, at this time, expressions for U_i, U_e, and α as a function of E/n could not be found in the literature for the E/n range seen in this thruster. Equations 9 and 10 will be useful for setting bounds on V_o in the next section.

V. Electron Field Emission from the Cathode

In this section, an attempt is made to characterize the values of β_m, β, and A_e in the arcjet. Expressions for the above parameters will then be used, along with SEM photographs of the cathode tip, to determine if the field enhancement due to the surface roughness at the cathode tip can explain the observed MDBVs.

The Macroscopic Field Enhancement Factor

The macroscopic field enhancement factor is essentially a non-dimensional form of the macroscopic electric field at the cathode tip; it will be used to attempt to understand the differences in the breakdown characteristics of the various cathode tips. The macroscopic field enhancement factor, β_m, is defined as the maximum macroscopic electric field at the cathode tip divided by V/d. Unlike the other parameters listed above, β_m can be calculated very accurately because it is a function of macroscopic arcjet dimensions only. Note that for a given arcjet and cathode geometry, β_m is a function of electrode gap distance only: $\beta_m = \beta_m(d)$.

For a particular arcjet and cathode geometry, this factor is calculated by solving Laplace's equation for the potential profile within the entire arcjet. These calculations were performed using the electrostatic problem solver routines in ALGOR[26], a commercially available finite element analysis package. Once the potential profile inside of the arcjet was determined, the electric field at the cathode surface was determined by extrapolating internal electric field values to the surface.

Finite element grids were defined so as to maximize the grid density in the regions of highest electric field. Solutions were checked for accuracy by two methods: increasing the grid density and by varying the physical extent of the region examined. The first method insured that the electric field was accurately represented with the grid density

used. The second method confirmed that the solution near the cathode tip was not changed by, for instance, extending the grid farther down the nozzle. Grid refinement reduced the solution uncertainty of the extrapolated electric field to less than a few percent; further grid refinement, while desirable, would have required computer RAM beyond that available (4 MB). Uncertainties due to the extent of the physical domain were small, less than 1%.

The above methods were used to calculate β_m as a function of cathode tip radius and electrode gap distance. For all cases, that the maximum electric field was located at the very tip of the cathode, on the centerline. Figure 14 shows a plot of β_m versus the radius of curvature of the tip for the

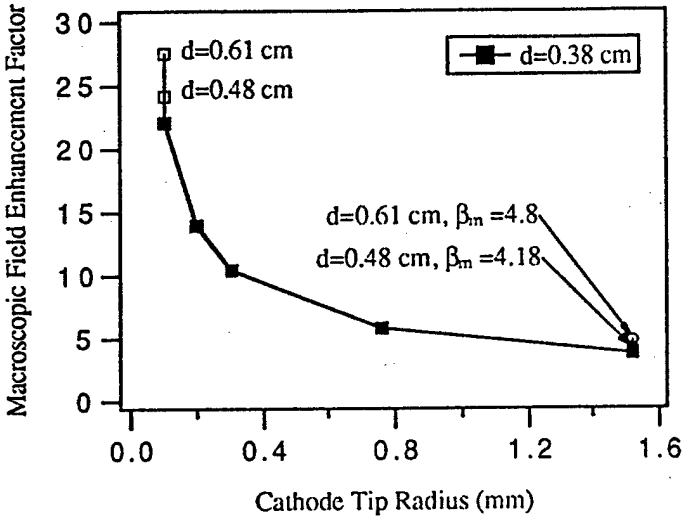

Figure 14: The effect of cathode tip radius on the macroscopic field enhancement factor.

high power arcjet geometry with an electrode gap distance of 0.38 cm. The cathode tip radius was chosen to range from 1.52 mm (the round tip cathode) to 0.1 mm corresponding roughly to the sharp tip cathode. At these two limits, β_m was also calculated at the other two electrode gap distances (0.48 cm and 0.61 cm). Note that at the microscopic level, the tip of the sharp tip cathode was actually somewhat flat, due to fabrication limitations, with a tip diameter of about 0.2 mm. No attempt was made to calculate β_m for the flat tip cathode due to the uncertainty in the radius of curvature at the edge of the flat region.

Figure 14 indicates that field emission can be significantly enhanced by sharpening the cathode tip, resulting in a lower MDBV (unless $V_{bo}/V' >> t_s$). By comparing the round tip characteristic (figure 6) with the sharp tip characteristic (figure 8), assuming identical surface roughness, this effect is seen only at the largest electrode gap distance. It is difficult to explain any of the differences between the cathode tips by differences in their field emission characteristics. Apparently, the problem with such an interpretation in the high power arcjet is that the breakdown formation process is also dependent on the macroscopic cathode tip shape.

A better idea of the relative magnitudes of the statistical and formative time lags can be obtained by examining breakdown characteristics at a fixed cathode tip shape. The strong variation of the MDBV with mass flow rate (figures 6-9) and voltage ramp rate (figure 11) indicate that the MDBV is closely coupled with the breakdown formation process. The variation in MDBV with mass flow rate is much more than can be explained by the variation of V_{bo}, and the drastic reduction in V_b with just a one order of magnitude decrease in V' cannot be explained by the variation in V_o. In figure 12, the strong effect of the cathode surface state on the MDBV indicates that the characteristic time required for an electron to be emitted from the cathode is also a significant factor in determining the MDBV. From these results it is concluded that the statistical time lag and the formative time lag are both significant in determining the MDBV in the high power ammonia arcjet.

The Determination of β and A_e

The determination of β and A_e is an active topic in vacuum breakdown phenomenon research[24]. There are two distinct categories of enhanced electron field emission mechanisms. The first mechanism links enhanced field emission to microprotusions emanating from the cathode surface (the projection model), and the second to the presence of very thin dielectric layers on the cathode surface[24,27,28]. In this paper, the validity of the projection model is investigated, especially because it appears logical that this will be the dominant mechanism due to the rough surface of the cathode tip.

The field enhancement factor is a function of the shape of the projection only, and has been calculated for various projection shapes[23,29]. For a cylindrical protrusion of height h, with a hemispherical tip of radius r [29]:

$$\beta = \frac{h}{r} + 2 \qquad (11)$$

Equation 11 also represents the field enhancement by a sphere of radius r, connected to the surface by a infinitesimal wire of length h. This expression represents the maximum field enhancement of any projection with tip radius r and height h. The field enhancement factor has also been calculated for sharp cones and spheroidal projections[23,29] to have a $\beta \sim h/r$ for $h/r >> 1$. As the aspect ratio of the projectile is reduced, for a given h and r, the field enhancement factor is significantly reduced. Other factors also affect the β of a projection, such as the electrode gap distance and the density of the projections on the surface. When the height of a projection is on the order of the spacing between electrodes, the β of the projection is reduced from its $d/h >> 1$ value[24]. In the high power arcjet, the effect of electrode gap distance on β is expected to be negligible because $d/h >> 1$ for the projections seen on the cathode surfaces. Projections in close proximity of each other will also reduce the field enhancement factors of each of the projections[30,31]. Such an effect will impact the field enhancement when the spacing between projections is on the order of their size.

The effective emission area for a single projection is

related to β by the following equation[32]:

$$A_e \sim 2\pi \frac{h^2}{\beta^2}$$

This equation is good for order of magnitude estimates of the emission area and reflects the common situation where field emission is dominated by a single high-β source. Since it appears that the arcjet cathode surface will provide a large number of high-β emission sites, the above equation can be multiplied by some factor N related to the number of emission sites. It has been shown, experimentally[32] and theoretically[33], that electron emission from multiple high-β sites still obeys the Fowler-Nordheim law (equation 5) with the appropriate value of A_e, and β taken to be a weighted average of the β's of all of the sites. In the arcjet, it is expected that field emitted electrons will initiate from many high-β sites. This is justified by the general observation of surface roughness on the cathode tip, and the identification of many projections with a scanning electron microscope. Furthermore, the assumption of only one dominate emitter on the cathode surface is not realistic considering that the MDBV is not significantly altered by the many 15 A, 100 μsec arcs associated with a single MDBV measurement, or even by an actual firing of the arcjet[3].

The Evaluation of the SEM Photographs

In this section, a survey of the round tip cathode surface with a scanning electron microscope, along with the breakdown data and equation 8, are used to determine if the projections on the surface can explain the observed MDBVs. Due to time limitations, an extensive survey of only the round tip cathode was performed; it was chosen because it is the only cathode for which β_m is known very accurately.

Shown in figure 15 is a plot of the effective emission area as a function of the field enhancement factor for the round tip cathode (d=0.38 cm, V_{bo} = 820 V, β_m =3.75, V' = 25 kV/μsec, ϕ=3.5 eV, T=298K). The above parameters correspond to figure 6, at a mass flow rate of 70 mg/sec and a MDBV of 4.3 kV. The smallest electrode gap distance and mass flow rate were used because while studying an electron emission mechanism, it was desirable to minimize the influence of the formation process on the MDBV. The conclusion reached in this section will not change at larger ṁ or d. The upper limit of the effective emission area was assumed to be 1 cm^2 which is on the order of the entire cathode tip area; the lower limit was assumed to be 10^{-13} cm^2. Near the lower limit, A_e is becoming on the order of atomic dimensions where the emission current density is seriously reduced, such that equation 5 is no longer applicable[23]. In this figure, the upper limit of V_o is taken to be the measured MDBV, corresponding to the case where the breakdown formation process is practically instantaneous once the electron is emitted from the cathode, ($V_{bo}/V' >> t_f$). The lower limit of was taken to be V_o = 1000 V corresponding to the case where $V_{bo}/V' >> t_s$, such that V_o is not much greater than V_{bo}. Finally, in an effort to obtain the lower limit on β, the cathode work function was taken to be 3.5 eV corresponding to a clean surface of 2% thoriated tungsten. Figure 15 shows that although A_e is not known, at the very minimum a β ~ 200-300 is required to maintain consistency between the projection model for enhance field emission and the MDBV measurements. From equation 11, field enhancement factors in this range correspond to projections with relatively high aspect ratio, and height to tip radius ratios on the order of 100.

With a scanning electron microscope, the tip of the round tip cathode was randomly searched for microscopic projections on its surface. The total coverage of the scan was estimated to be on the order of 1% of the total tip area. A 1% coverage is expected to give a good representation of the projection shapes on the cathode surface, because of the large number of emission sites expected to be on the surface. The majority of the structure seen on the cathode surface were crater formations (see figures 16a and 16b). Crater formations consist of many solidified splashes of molten tungsten situated upon each other; the observed upper limit of β for the projections associated with these formations was less than 10. Aside from the crater formations, many projections with sizes on the order of a few micrometers were

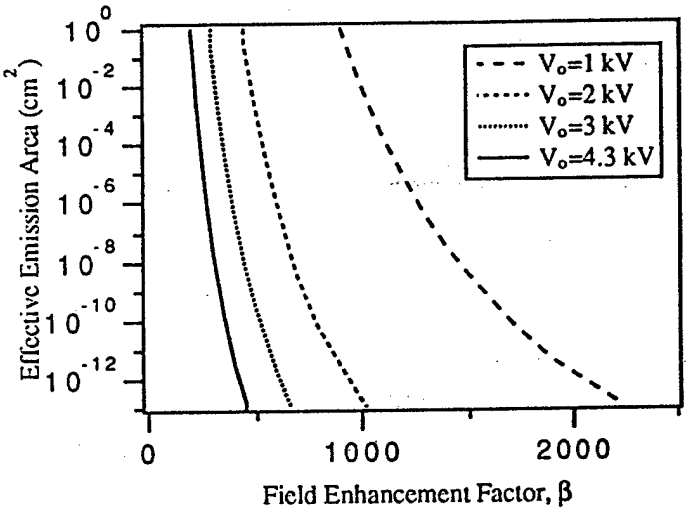

Figure 15: The range of β and A_e on corresponding to various V_o for the round tip cathode (d =0.38 cm, V_{bo} =820 V, β_m =3.75, V'=25 kV/μsec, ϕ=3.5 eV, T=298 K).

observed (see figures 16c and 16d). For projections such as these, an upper limit of β (β_{max}) can be estimated with equation 11 by letting r equal smallest radius of curvature at the tip of the projection, and h equal to the tallest height. Within the entire scan of the cathode tip, no projection was found with a β_{max} greater than 25. This result indicates that the projection model for enhanced field emission cannot alone explain the MDBV data for the round tip cathode in the ammonia arcjet.

One explanation for this discrepancy is that these high aspect ratio projections do indeed exist on the cathode surface, and through the handling of the cathode after the breakdown tests, were somehow eliminated from the cathode surface. Such an explanation may be correct, because although the cathodes were handled with care (a SEM analysis of the cathode tips was planned as part of these tests), human

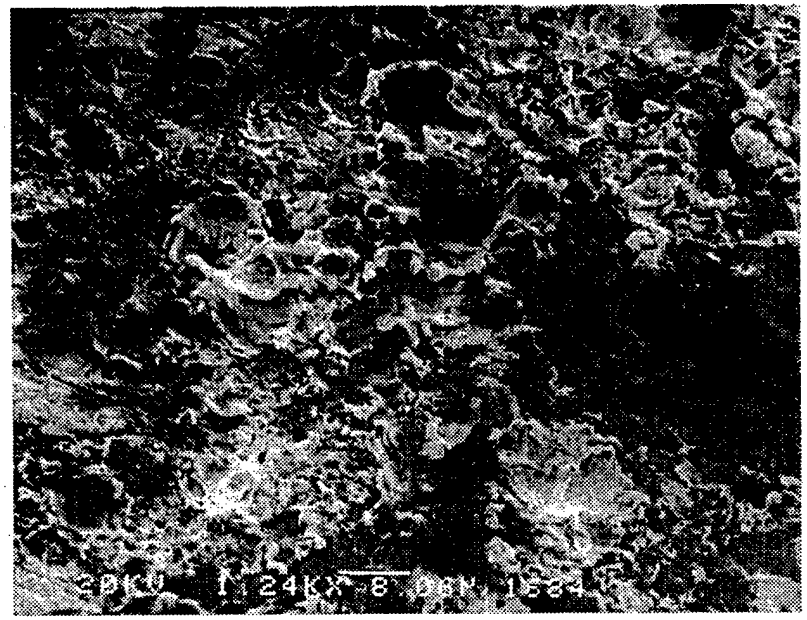

(a) 1 cm = 8.06μm

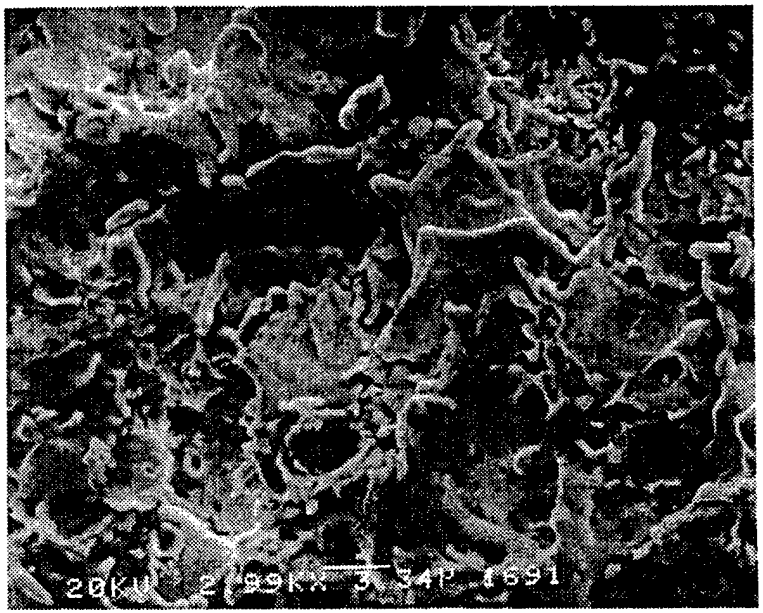

(b) 1 cm = 3.34μm

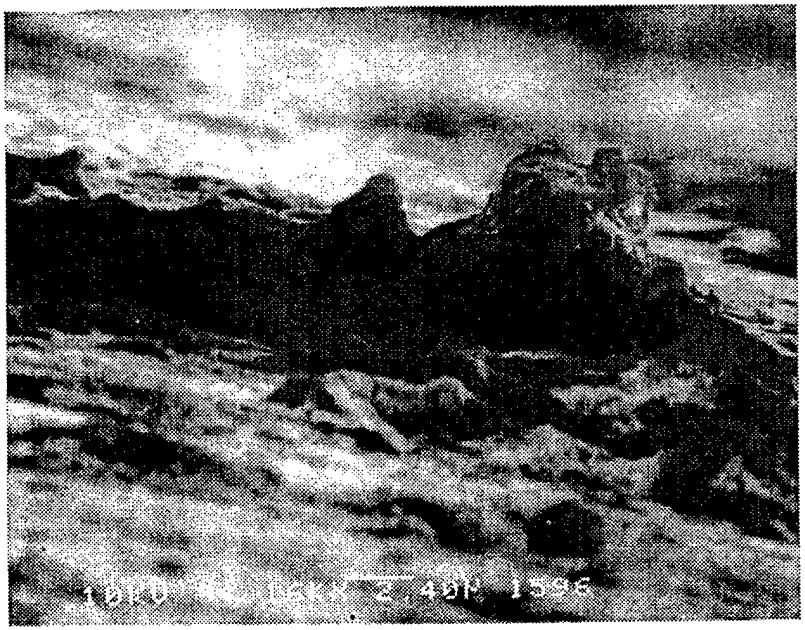

(c) 1 cm = 2.40μm

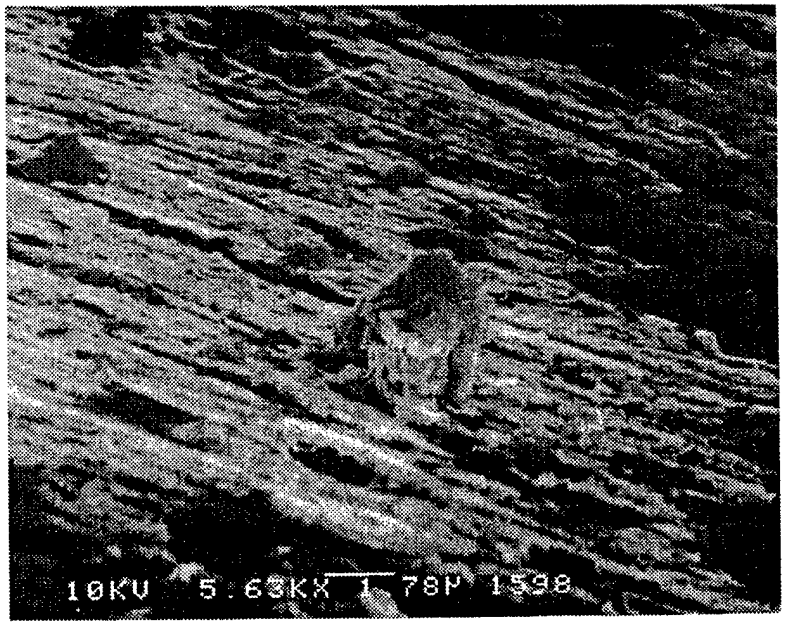

(d) 1 cm = 1.78μm

Figure 16

contact with the cathode tips was allowed. This explanation also has serious shortcomings. Firstly, the lack of an explanation for how these projections formed on a newly machined cathode that had been conditioned for ten minutes only once. Secondly, past reports of SEM studies of the cathode tip make no mention of any microscopic, high aspect ratio projections on the cathode surface in both 1 kW arcjets[3,34] and in 30 kW arcjets[35,36].

The more probable explanation for the discrepancy is that the mechanism for enhanced field emission is one that is dependent on dielectric layers on the cathode surface[24,28], such as the field-induced hot-electron emission mechanism[27]. It is very common to have field enhancement factors in the high hundreds for these type of mechanisms[24,27,28]; and is most probable that these mechanisms work in conjunction with the field enhancement due to microprojections, to produce very high field enhancement factors that can explain the observed MDBVs. Such mechanisms also provide an excellent explanation for MDBV sensitivity on the state of the cathode surface.

Another issue associated with these results is just how does the round tip cathode, which had never been fired in the arcjet, reflect actual arcjet cathode tips? Certainly, large whiskers have been observed on the cathodes of 30 kW arcjets[35,36], which have corresponding field enhancement factors on the order of 100. However, not all cathodes exhibit whisker growth; in fact, whiskers on 1 kW arcjet cathodes have not been observed at all[34]. A preliminary SEM analysis of the tips of the burned-in cathode #2 and the sharp tip cathode also resulted in no sightings of very sharp projections, although the tip coverage of these scans was a few orders of magnitude less than that of the round tip cathode. Analysis of the unpublished SEM photographs associated with the study of reference 36, resulted in the sighting of projections with a β as high as 50. Considering the lack of evidence for the microscopic high aspect ratio projections on actual cathode surfaces, and the fact that β's in the high hundreds or even thousands are required to explain the MDBVs in high power arcjets, it also appears that some mechanism, other than microprojections, is responsible for emission of the initial electron required for the ignition of a high power arcjet in a vacuum chamber.

If the enhanced emission process is due to dielectric surface layers on the cathode surface, another issue to be resolved later, is to identify the source of the insulator atoms and/or particles. Possible options include: insulator material internal to the arcjet, the adsorption and/or chemical reaction between the propellant and cathode materials, the adsorption and/or chemical reaction between residual gases such as oxygen, nitrogen, and pump oil fragments with cathode materials, and dust particles. The last two options certainly have implications concerning the ground testing of arcjet ignition. More research is required to resolve this issue and those discussed above.

VI. Conclusions

The primary objective of this work was to identify methods to reduce the mean dynamic breakdown voltage (MDBV) of the ammonia propellant in the ESEX 26 kW arcjet. The approach to this objective was to establish a test matrix to investigate the influence of mass flow rate, electrode gap distance, cathode tip shape, and voltage ramp rate on the MDBV. Only the mass flow rate and voltage ramp rate were observed to significantly affect the MDBV; the MDBV was observed to rise as either of these parameters were increased. These test results provided the bases for the start circuit redesign for the ESEX flight experiment, and also represent an initial data base of breakdown characteristics in high power ammonia arcjets.

The second objective of this work was to identify the mechanisms associated with propellant breakdown in an arcjet. Work on this objective is currently in progress, but preliminary results, as applied to propellant breakdown in the high power ammonia arcjet, include:

1. A framework for investigating breakdown mechanisms in an arcjet was established. This framework provides explanations for the strong dependence of the MDBV on the voltage ramp rate and the mass flow rate, among others.

2. Electron field emission is the dominant source of the initial electrons required to initiate breakdown. The mechanism associated with the breakdown formation process could not be identified in the high power ammonia arcjet.

3. A combination of a model, the calculation of electric field contours inside of the arcjet, and SEM photographs of a cathode tip indicate that the projection model for enhance field emission cannot alone account for the mean dynamic breakdown voltages observed in the high power arcjet. This indicates that dielectric surface layers on the cathode tip are most likely responsible for the enhanced field emission required to explain the observed MDBVs.

4. More research is required to resolve the many issues associated with breakdown mechanisms in the arcjet. The PL research program is in the process of addressing these issues.

Acknowledgements

The authors would like to acknowledge the following individuals for their helpful comments on the experimental work: Joe Cassady and Andy Hoskins of the Rocket Research Company; Bob Kay of Pacific Electro Dynamics; Mary Kriebel and John Biess of TRW. We would also like to thank Jim King (PL/RKFE) for performing the scanning electron microscopy of the cathode tips, and Jay Polk of JPL for providing access to the breakdown data obtained in the lifetest discussed in reference 5.

References

1. Jones, J.M., Sanks, T.M., and Raygor, B.L., "The USAF Electric Propulsion Systems Activities", AIAA Paper No. 92-3702, 1992.

2. Presentation given at TRW by Joe Cassady of the Rocket Research Company, Nov. 12, 1992.

3. Sarmiento, C.J. and Gruber, R.P., "Low Power Arcjet Thruster Pulse Ignition", AIAA Paper No. 87-1951, 1987.

4. Pencil, E.J., et. al., "Dependence of Hydrogen Arcjet Operation on Electrode Geometry", AIAA Paper No. 92-3530, 1992.

5. Polk, J.E., Goodfellow, K.D., and Pless, L.C., "Ammonia Arcjet Engine Behavior in a Cyclic Endurance Test at 10 kW", 43rd Congress of the International Astronautical Federation, Paper No. IAF-92-0612, 1992.

6. Wong, S.P., "Testing of the 30 kW Arcjet PCU Starter using the Shorting Switch Approach", 22nd International Electric Propulsion Conference, Viareggio, Italy, IEPC Paper No. 91-030, 1991.

7. Wong, S.P., "Testing of a 30 kW Arcjet PCU with Arcjet Thrusters", 22nd International Electric Propulsion Conference, Viareggio, Italy, IEPC Paper No. 91-070, 1991.

8. Hamley, J.A., et. al., "10 kW Power Electronics for Hydrogen Arcjets", NASA TM-105614, 1992.

9. Tilley, D.L., "Propellant Breakdown Mechanisms in an Arcjet", to be presented at the 23rd International Electric Propulsion Conference in Seattle, WA, Sept. 1993.

10. Deininger, W.D., Chopra, A., Goodfellow, K.D., "Cathode Erosion Tests for 30 kW Arcjets", AIAA Paper No. 89-2264, 1989.

11. Cassady, R.J., Lichon, P.G., and King, D.Q., "Arcjet Endurance Test Program", Technical Report AL-TR-90-069, Phillips Laboratory, Edwards A.F.B., CA, March 1991.

12. Personal communication with Bob Kay of Pacific Electro Dynamics, Redmond, WA., December 1992.

13. Schonhuber, M.J., "Breakdown of Gases Below the Paschen Minimum: Basic Design Data of High-Voltage Equipment", IEEE Trans. on Power App. and Systems, Vol. PAS-88, 1969, pp. 100-107.

14. Personal communication with John Hamley of the NASA Lewis Research Center, Nov. 92.

15. Personal communication with Jay Polk of the Jet Propulsion Laboratory, April 1993 (unpublished dynamic breakdown voltage data from the test of reference 5).

16. Morgan, C.G., "Irradiation and Time Lags" in Electrical Breakdown of Gases, Meck, J.M. and Craggs, J.D., editors, John Wiley & Sons, 1978, pp. 655-688.

17. Kunhardt, E.E. and Luessen, L.H., editors, Electric Breakdown and Discharges in Gases: Part A: Fundamental Processes and Breakdown, Plenom Press, 1983.

18. Vincenti, W.G. and Kruger, C.H., Introduction to Physical Gas Dynamics, Robert E. Krieger Publishing Company, Malabar, FL, 1965, pp. 296-300.

19. Swanson, L.W. and Bell, A.E., "Recent Advances in Field Electron Microscopy of Metals" in Advances in Electronics and Electron Physics, edited by Marton, L., Academic Press, 1973, pp. 193-309.

20. Dyke, W.P. and Dolan, W.W., "Field Emission", in Advances in Electronics and Electron Physics, edited by Marton, L., Academic Press, 1956, pp. 89-185.

21. Murphy, E.L. and Good, R.H., "Thermionic Emission, Field Emission, and the Transition Region", Phys. Rev., Vol. 102, 1956, pp. 1464-1473.

22. Burgess, R.E., Kroemer, H., Houston, J.M., "Corrected Values of Fowler-Nordheim Emission Functions v(y) and s(y)", Phys. Rev., Vol. 90, 1953, p. 515. Note that t(y) = [4s(y)-v(y)]/3.

23. Chatterton, P.A., "Vacuum Breakdown" in Electrical Breakdown of Gases, Meek, J.M. and Craggs, J.D., editors, John Wiley & Sons, 1978, pp. 129-208.

24. Noer, R.J., "Electron Field Emission from Broad-Area Electrodes", Appl. Phys., Vol. A28, 1982, pp. 1-24.

25. Brown, S.C., Introduction to Electrical Discharges in Gases, John Wiley and Sons, 1966.

26. Algor Finite Element Analysis Software, Algor, Inc., Pittsburgh, PA.

27. Latham, R.V., "A New Perspective of the Origin of Prebreakdown Electron Emission Processes", IEEE Trans. on Elect. Insulation, Vol. 23, 1988, pp. 9-16.

28. Latham, R.V., "Prebreakdown Electron Emission", IEEE Trans. on Elect. Insulation, Vol. EI-18, 1983, pp. 194-203.

29. Chatterton, P.A., "A Theoretical Study of Field Emission Initiated Vacuum Breakdown", Proc. Phys. Soc., Vol. 88, 1966, pp.231-245.

30. Lewis, T.J., "High Field Electron Emission from Irregular Cathode Surfaces", J. Appl. Phys., Vol. 26, 1955, pp. 1405-1410.

31. Nordgard, J.D., "On the Optimization of Electron-Emitting Arrays", J. Appl. Phys., Vol. 48, 1977, pp. 3042-3049.

32. Farrall, G.A., "Numerical Analysis of Field Emission and Thermally Enhanced Emission From Broad-Area Electrodes in Vacuum", J. Appl. Phys., Vol. 41, 1970, pp. 563-571.

33. Schroder, D.K. and Thomas, R.N., "Experimental Confirmation of the Fowler-Nordheim Law for Large-Area

Field Emitter Arrays", Appl. Phys. Lett., Vol. 23, 1973, pp. 15-16.

34. Curran, F.M., Haag, T.W., Raquet, J.F., "Arcjet Cathode Phenomena", Proceedings of the JANNAF Propulsion Meeting, Vol. 1, May 1989, pp. 349-366.

35. Pivirotto, T.J. and Deininger, W.D., "Electrode Erosion in Steady-State Electric Propulsion Engines", 20th International Electric Propulsion Conference, Germany, IEPC Paper No. 88-074, 1988.

36. Maher, J. and Andrews, J., "The Analysis of Arcjet Cathodes by Scanning Electron Microscopy", AIAA Paper No. 91-2452, 1991.